

## Charge storage characteristics of Mo nanocrystal dependence on Mo oxide reduction

Chao-Cheng Lin, Ting-Chang Chang, Chun-Hao Tu, Wei-Ren Chen, Chih-Wei Hu, Simon M. Sze, Tseung-Yuen Tseng, Sheng-Chi Chen, and Jian-Yang Lin

Citation: *Applied Physics Letters* **93**, 222101 (2008); doi: 10.1063/1.3039065

View online: <http://dx.doi.org/10.1063/1.3039065>

View Table of Contents: <http://scitation.aip.org/content/aip/journal/apl/93/22?ver=pdfcov>

Published by the [AIP Publishing](#)

---

### Articles you may be interested in

[Physical and electrical characteristics of atomic layer deposited TiN nanocrystal memory capacitors](#)  
*Appl. Phys. Lett.* **91**, 043114 (2007); 10.1063/1.2766680

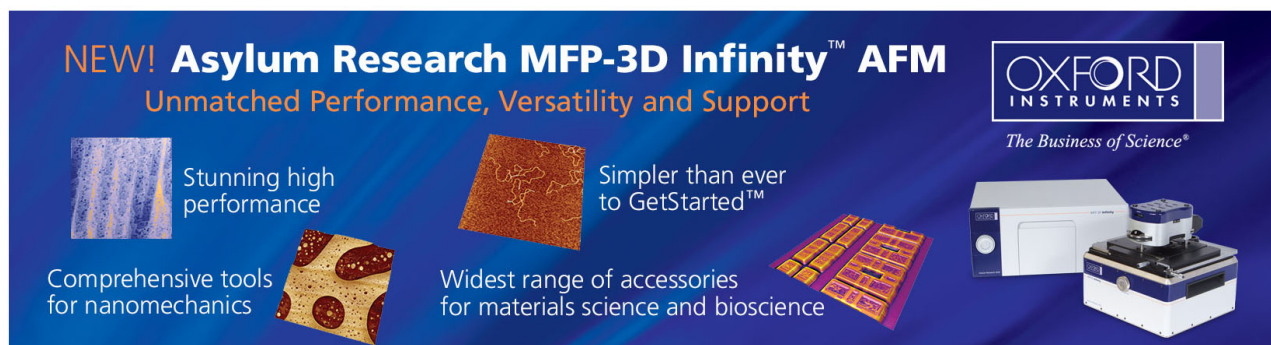
[Highly thermally stable TiN nanocrystals as charge trapping sites for nonvolatile memory device applications](#)  
*Appl. Phys. Lett.* **86**, 123110 (2005); 10.1063/1.1890481

[Effect of germanium concentration and tunnel oxide thickness on nanocrystal formation and charge storage/retention characteristics of a trilayer memory structure](#)  
*Appl. Phys. Lett.* **83**, 3558 (2003); 10.1063/1.1615840

[Observation of memory effect in germanium nanocrystals embedded in an amorphous silicon oxide matrix of a metal-insulator-semiconductor structure](#)  
*Appl. Phys. Lett.* **80**, 2014 (2002); 10.1063/1.1459760

[Enhancement on field-emission characteristics of diamondlike coated Mo substrates by redox process](#)  
*J. Vac. Sci. Technol. B* **19**, 1739 (2001); 10.1116/1.1394726

---

The advertisement features a dark blue background with white and orange text. At the top left, it reads 'NEW! Asylum Research MFP-3D Infinity™ AFM' in large white letters, followed by 'Unmatched Performance, Versatility and Support' in orange. To the right is the Oxford Instruments logo with the tagline 'The Business of Science®'. Below the text are four images: a blue textured surface, a brown textured surface, a yellow and red patterned surface, and a photograph of the MFP-3D Infinity AFM instrument. Text descriptions are placed around these images: 'Stunning high performance' (top left), 'Simpler than ever to GetStarted™' (top right), 'Comprehensive tools for nanomechanics' (bottom left), and 'Widest range of accessories for materials science and bioscience' (bottom right).

## Charge storage characteristics of Mo nanocrystal dependence on Mo oxide reduction

Chao-Cheng Lin,<sup>1</sup> Ting-Chang Chang,<sup>2,a)</sup> Chun-Hao Tu,<sup>1</sup> Wei-Ren Chen,<sup>1</sup> Chih-Wei Hu,<sup>1</sup> Simon M. Sze,<sup>1</sup> Tseung-Yuen Tseng,<sup>1</sup> Sheng-Chi Chen,<sup>3</sup> and Jian-Yang Lin<sup>3</sup>

<sup>1</sup>Institute of Electronics, National Chiao Tung University, Hsin-Chu 300, Taiwan

<sup>2</sup>Department of Physics and Institute of Electro-Optical Engineering, Center for Nanoscience and Nanotechnology, National Sun Yat-Sen University, 70 Lien-hai Road, Kaohsiung 804, Taiwan

<sup>3</sup>Department of Opto-Electronic Engineering, National Yunlin University of Science and Technology, Yunlin 64002, Taiwan

(Received 17 July 2008; accepted 9 November 2008; published online 1 December 2008)

An oxygen incorporated Mo silicide was explored to form the Mo nanocrystals after rapid thermal annealing. Transmission electron microscopy showed the nanocrystals embedded in SiO<sub>x</sub>. Charge storage characteristics of Mo nanocrystals influenced by the Mo oxide and the surrounding oxide were investigated through x-ray photoelectron spectroscopy and the electrical measurement. X-ray photoelectron spectra analyses revealed the redox reaction in the oxygen incorporated Mo silicide layer after rapid thermal annealing. The memory window and retention were improved due to reduction in Mo oxide. © 2008 American Institute of Physics. [DOI: 10.1063/1.3039065]

In recent years, discrete nanocrystals composed floating gate nonvolatile memory structure has been widely investigated as a candidate for next generation nonvolatile memory because charges stored in lateral isolated nanocrystals instead of continuous conducting polycrystalline silicon layer are more immune to the local defect chain in the tunnel oxide.<sup>1-4</sup> Many materials, such as Si, Ge, Ni, and Co, have been proposed to fabricate nanocrystal memory.<sup>2-6</sup> Because of benefits on strong coupling, deep quantum well, and large density of state, metal nanocrystals have recently received much attention for research.<sup>5-7</sup> However, the use of metal must take thermal stability issue into account because the metal diffusion into or chemical reaction with tunnel oxide during the memory fabrication process will compromise the performance of the memory structure.<sup>6</sup> Mo is an attractive candidate because of its high work function, compatible with complementary metal-oxide-semiconductor process and high thermal stability.<sup>8</sup>

In this study, nonvolatile memory characteristics of Mo nanocrystals embedded in SiO<sub>x</sub> were investigated by thermal annealing oxygen incorporated Mo silicide layer. Our experiment results show that the Mo oxide was formed in the as-deposited layer. Lee *et al.*<sup>9</sup> proposed that the formation of metal oxide during the nanocrystal fabrication process reduces charge storage ability. To reduce the metal oxide, they need to perform a long-term thermal treatment in hydrogen ambience. In our investigation, we found that the Mo oxide was reduced after a critical annealing temperature, and this result improved the charge storage ability of Mo nanocrystal memory cell.

The memory cell structures were fabricated on a 6 in. *p*-type Si substrate. A 5-nm-thick dry oxide (tunnel oxide) was thermally grown at 950 °C on the substrate in a horizontal furnace after the substrate was cleaned by Radio Corporation of America process. An 8-nm-thick oxygen incorporated Mo silicide layer was deposited on the tunnel oxide by cosputtering Mo and Si targets in Ar (24 SCCM)/O<sub>2</sub>

(2 SCCM) (SCCM denotes standard cubic centimeter per minute at STP) ambience. Subsequently, a 30-nm-thick silicon dioxide (blocking oxide) was deposited on the layer by plasma enhanced chemical vapor deposition at 300 °C. Thermal annealing process at 800 and 900 °C was performed in N<sub>2</sub> for 60 s to investigate the temperature's influence on the memory characteristics of oxygen incorporated silicide layer. Finally, a 500-nm-thick Al gate patterned with shadow mask was evaporated by thermal coater to form the memory structures. Transmission electron microscopy (TEM) and x-ray photoelectron spectroscopy (XPS) were used to analyze the microstructure and chemical composition of nanocrystals and their surrounding oxide. Electrical characteristics of the capacitance-voltage (*C-V*) hysteresis were measured by HP4284 Precision LCR Meter with frequency of 1 MHz.

Figure 1 shows the plane-view TEM image of 900 °C

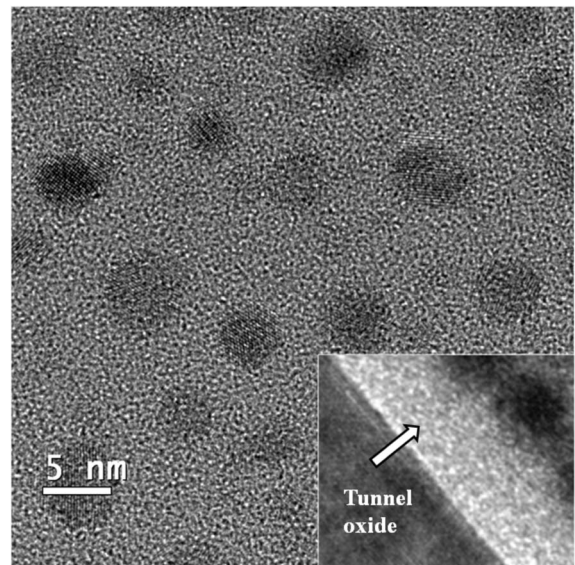


FIG. 1. Plane-view and cross-sectional (inset) TEM analyses of Mo nanocrystals embedded in SiO<sub>x</sub>.

<sup>a)</sup>Electronic mail: tcchang@mail.phys.nsysu.edu.tw.

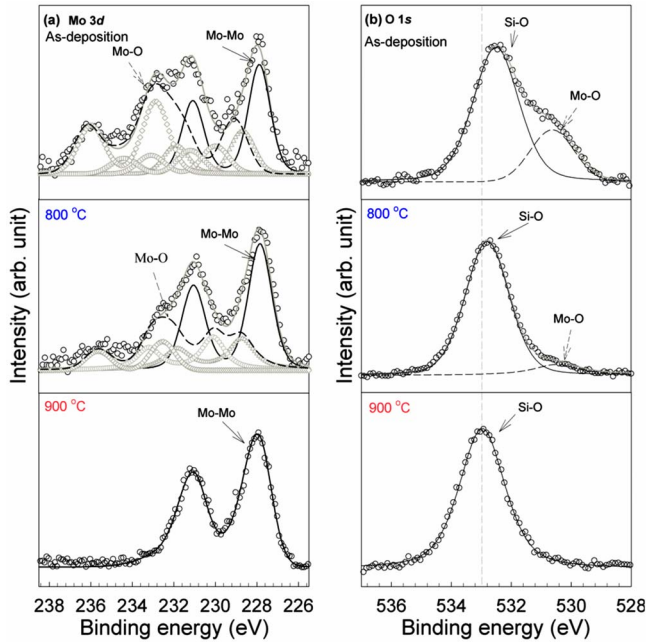


FIG. 2. (Color online) (a) Mo 3d and (b) O 1s core-level spectra of the oxygen incorporated Mo silicide layer for as-deposited, 800, and 900 °C annealed samples. The Mo–O bonds in Mo 3d spectra originated from various oxidation states, Mo<sup>3+</sup> (triangle), Mo<sup>4+</sup> (gray circle), Mo<sup>5+</sup> (square), and Mo<sup>6+</sup> (diamond).

sample to observe the microstructure of nanocrystals. The average diameter of the nanocrystals is approximately 4 nm and the area density of the nanocrystals is estimated to be about  $1.01 \times 10^{12} \text{ cm}^{-2}$ . The cross-sectional TEM image (inset of Fig. 1) shows a clear interface of tunnel oxide. Besides, secondary ion mass spectra results (unshown) exhibit that the position of Mo atom was unchanged between the tunnel oxide and the blocking oxide after 900 °C annealing. This is important because metal atoms that diffuse into tunnel oxide would deteriorate the reliability of the nonvolatile memory.

To investigate the chemical composition of oxygen incorporated Mo silicide layer after annealing, the XPS analyses were performed by using an Al K $\alpha$  (1486.6 eV) x-ray. Figures 2(a) and 2(b) show the XPS Mo 3d and O 1s core-level spectra, respectively. The Mo 3d spectra of as-deposited sample show Mo–Mo and Mo–O bonds indicating the existence of metallic Mo and Mo oxides that correspond to various oxidation states (Mo<sup>6+</sup>, Mo<sup>5+</sup>, Mo<sup>4+</sup>, and Mo<sup>3+</sup>).<sup>10–13</sup> The 800 °C annealed samples also contain metallic Mo and Mo oxides, but the area of Mo–O bonds is less than that for as-deposited sample in Fig. 2(a). After the 900 °C annealing, there is only metallic Mo in the oxygen incorporated layer, as shown in Fig. 2(a). The XPS Mo 3d shows that the Mo oxides were reduced as the annealing temperature was increased. In Fig. 2(b), the O 1s spectra of as-deposited and 800 °C annealed samples show Mo–O and Si–O bonds. The XPS peak of Si–O bond for as-deposited sample is less than 533.4 eV (the binding energy of SiO<sub>2</sub>), which indicates that the oxide around Mo nanocrystals is deficient (SiO<sub>x</sub>,  $x < 2$ ) in the oxygen incorporated layer. There are only Si–O bonds, and the peak position of Si–O bonds shift toward higher binding energy for the sample after 900 °C annealing. According to literature, the increment of O 1s binding energy is attributed to the oxygen bonding with

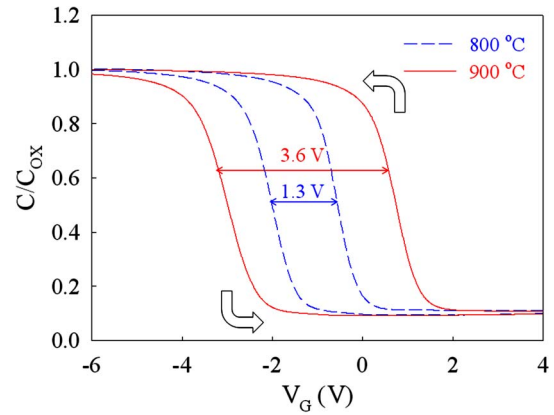


FIG. 3. (Color online) The comparison of the C–V curves of the samples annealed at 800 and 900 °C.

deficient silicon oxide.<sup>14</sup> The XPS results show that a redox between MoO<sub>x</sub> and SiO<sub>x</sub> occurred during the thermal annealing process. For the redox behavior in the oxygen incorporated Mo silicide layer, we consider that the formation energy of Si oxide (–750 kJ/mole) is larger than that of Mo oxide (–450 kJ/mole).<sup>15</sup> Therefore, the oxygen of Mo oxides prefers to bond with Si than Mo during the thermal annealing at 900 °C, which results in the reduction in Mo oxide and improved the quality of SiO<sub>x</sub>.

Figure 3 shows the comparison of the C–V curves for the 800 and 900 °C annealed samples. The curves were obtained after the gate voltage swept from inversion to accumulation region of the substrate (from 9 to –11 V) and the reverse (from –11 to 9 V). The hysteresis loop of the samples is counterclockwise due to substrate injection through the tunnel oxide. We note that the memory window (the width of the loop) for 900 °C annealed sample is twice larger than that for 800 °C one. According to XPS results, we speculate that the larger memory window for 900 °C annealed sample was due to the reduction in Mo oxide that was proposed as a semiconductorlike metal oxide. Therefore, the Mo oxide has lower density of state than metallic Mo for the charge storage.

Figure 4 shows the retention behavior of 800 and 900 °C samples. The retention was measured by stress voltage of 10 V on gate electrode for 5 s. The memory window is obtained by comparing the C–V curves of a charged state

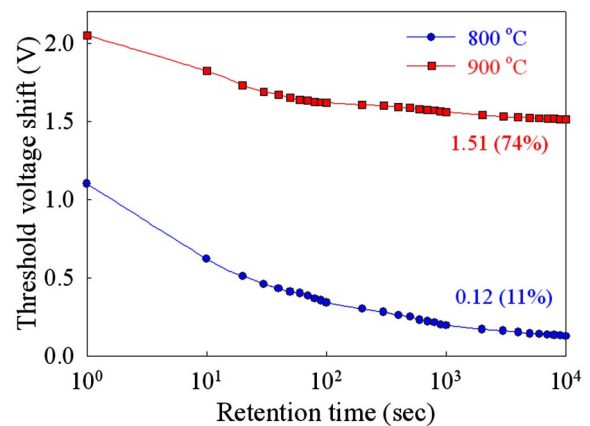


FIG. 4. (Color online) the retention behavior of samples annealed at 800 °C (remained charges of 11%) and 900 °C (remained charges of 74%).

to a quasineutral state. It can be found that the memory window of 800 °C annealed sample decreased significantly and remained ~11% after  $10^4$  s. In contrast, the retention of 900 °C annealed sample remained ~74%. From the XPS results (Fig. 2), the different retention behavior was considered to be due to the quality of the surrounding oxide. When charges are stored in the nanocrystals, the stored charges can escape laterally through the traps in the surrounding oxide. If the tunnel oxide has a leakage path, the lateral escaped charges will leak into the substrate. Because the surrounding oxide quality of 900 °C annealed sample was improved by the redox reaction between Mo oxide and  $\text{SiO}_x$ , more charges can remain in the Mo nanocrystals.

In conclusion, Mo nanocrystals were fabricated for non-volatile memory application through thermal annealing of oxygen incorporated Mo silicide layer. The average size and density of Mo nanocrystals were estimated to be about 4 nm and  $1 \times 10^{-12}$ , respectively. The XPS results indicate the existence of Mo oxide and  $\text{SiO}_x$  in oxygen incorporated Mo silicide layer after 800 °C annealing, and the Mo oxide was reduced after 900 °C annealing. The 900 °C annealed sample has the better retention (74%) and the larger memory window (3.6 V) than the 800 °C one due to the reduction in Mo oxide.

This work was performed at National Nano Device Laboratories, Taiwan, R.O.C. The authors would like to ac-

knowledge the financial support of the National Science Council (NSC) under Contract Nos. NSC 96-2221-E-009-202-MY3, NSC 96-2112-M-110-013, and NSC-97-3114-M-110-001.

<sup>1</sup>S. Tiwari, F. Rana, K. Chan, H. Hanafi, W. Chan, and D. Buchanan, *Tech Dig. Int. Electron Devices Meet.* **1995**, 521.

<sup>2</sup>S. Tiwari, F. Rana, H. Hanafi, A. Hartstein, E. F. Crabbe, and K. Chan, *Appl. Phys. Lett.* **68**, 1377 (1996).

<sup>3</sup>J. D. Blauwe, *IEEE Trans. Nanotechnol.* **1**, 72 (2002).

<sup>4</sup>C. H. Tu, T. C. Chang, P. T. Liu, H. C. Liu, S. M. Sze, and C. Y. Chang, *Appl. Phys. Lett.* **89**, 16215 (2006).

<sup>5</sup>S. Tang, C. Mao, Y. Liu, D. Q. Kelly, and S. K. Banerjee, *IEEE Electron Device Lett.* **54**, 433 (2007).

<sup>6</sup>J. Dufourcq, P. Murb, M. J. Gordonc, S. Minoretb, R. Copparda, and T. Baron, *Mater. Sci. Eng., C* **27**, 1496 (2007).

<sup>7</sup>Z. Liu, C. Lee, V. Narayanan, G. Pei, and E. C. Kan, *IEEE Electron Device Lett.* **49**, 1606 (2002).

<sup>8</sup>T.-L. Li, W. L. Ho, H. B. Chen, H. C. H. Wang, C. Y. Chang, and C. Hu, *IEEE Trans. Electron Devices* **53**, 1420 (2006).

<sup>9</sup>C. Lee, J. H. Kwon, J. S. Lee, Y. M. Kim, Y. Choi, H. Shin, J. Lee, and B. H. Sohn, *Appl. Phys. Lett.* **91**, 153506 (2007).

<sup>10</sup>C. B. Roxlo, H. W. Deckman, J. Gland, S. D. Cameron, and R. R. Chianelli, *Science* **235**, 1629 (1987).

<sup>11</sup>Y. C. Lu and C. R. Clayton, *Corros. Sci.* **29**, 927 (1989).

<sup>12</sup>T. S. Sian and G. B. Reddy, *Sol. Energy Mater. Sol. Cells* **82**, 375 (2004).

<sup>13</sup>J. F. Moulder, W. F. Stickle, P. E. Sobol, and K. D. Bomben, *Handbook of X-ray Photoelectron Spectroscopy* (Perkin-Elmer, Minnesota, 1992).

<sup>14</sup>J. X. Wu, M. S. Ma, H. G. Zheng, H. W. Yang, J. S. Zhu, and M. R. Ji, *Phys. Rev. B* **60**, 17102 (1999).

<sup>15</sup>R. Mitra, *Int. Mater. Rev.* **51**, 13 (2006).